Understanding the switching-off mechanism in Ag^+ migration based resistively switching model systems

Xin Guo, Christina Schindler, Stephan Menzel, and Rainer Waser

Citation: Appl. Phys. Lett. **91**, 133513 (2007); doi: 10.1063/1.2793686
View online: https://doi.org/10.1063/1.2793686
View Table of Contents: http://aip.scitation.org/toc/apl/91/13
Published by the American Institute of Physics

Understanding the switching-off mechanism in Ag^+ migration based resistively switching model systems

Xin Guo[a] and Christina Schindler
Institut für Festkörperforschung, Forschungszentrum Jülich, 52425 Jülich, Germany and Center of Nanoelectronic Systems for Information Technology, Forschungszentrum Jülich, 52425 Jülich, Germany

Stephan Menzel
Institut für Werkstoffe der Elektrotechnik (IWE 2), RWTH Aachen, 52056 Aachen, Germany

Rainer Waser
Institut für Festkörperforschung, Forschungszentrum Jülich, 52425 Jülich, Germany; Center of Nanoelectronic Systems for Information Technology, Forschungszentrum Jülich, 52425 Jülich, Germany; and Institut für Werkstoffe der Elektrotechnik (IWE 2), RWTH Aachen, 52056 Aachen, Germany

(Received 30 July 2007; accepted 12 September 2007; published online 28 September 2007)

Different coplanar Pt/Ag structures were prepared by photolithography on SiO_2 substrates, and $Pt/H_2O/Ag$ cells were formed by adding de-ionized H_2O to the coplanar Pt/Ag structures. The $Pt/H_2O/Ag$ cell is utilized here as a model system, due to the feasibility of visual inspection of the switching process. Bipolar switching was achieved for the cell. Scanning electron microscopy (SEM) investigations demonstrated that the growth and dissolution of Ag dendrites are responsible for the resistive switching. The Ag dendrite morphology is proposed to be the origin of the asymmetrical dissolution during the switching-off process, hence the bipolar nature of the switching characteristics. © *2007 American Institute of Physics*. [DOI: 10.1063/1.2793686]

Resistive switching has been commonly observed in various oxides, e.g., Cu_xO,[1] NiO,[2,3] TiO_2,[4–6] $SrTiO_3$,[7–9] $BaTiO_3$,[10] $(Ba,Sr)TiO_3$,[11] $SrZrO_3$,[12] $La_{1-x}Sr_xMnO_3$,[13] and $Pr_{1-x}Ca_xMnO_3$,[14–16] as well as in higher chalcogenides, e.g., Ag or Cu doped Ge_xSe_{1-x},[17,18] Ag_2S,[19] and Cu_2S.[20] Quite diverse switching mechanisms have been proposed, based on thermal, electronic, and/or electrochemical effects. In particular, when one involved electrode metal is situated in the intermediate range of the electrochemical potential series and forms mobile cations, such as Ag^+ and Cu^+, bipolar switching characteristics are observed, and electrochemical redox processes are generally accepted to be responsible for the switching. The switching on is due to the electrochemical formation of metallic filaments in the ion-conducting chalcogenide phase, whereas the switching off is triggered by the dissolution of these filaments. While the switching-on process is understood quite well, a few general questions remain open for the switching-off process. In particular, how and where the rupture of metallic filaments is carried out is still unclear. When a high enough current is driven through the system, metallic filaments can definitely be ruptured by Joule heating. In this work, we deal with these questions: what causes the filament rupture in the low-current regime, and what causes the bipolar *I-V* characteristics, despite the chemical symmetry in the cell after switching-on?

Cells consisting of an oxidizable electrode (Ag), de-ionized water, and an inert electrode (Pt) were prepared in this work as model systems. To facilitate the observation of the switching processes, a coplanar structure, instead of the common metal-insulator-metal stack structure, was fabricated on SiO_2 substrates by photolithography. Sputtered Pt with a thickness of 200 nm was used as the inert electrode, and electron beam evaporated Ag with a thickness of 200 nm as the oxidizable electrode. The gaps between the Pt electrode and the Ag electrode were in the range of 0.6–100 μm. By adding a drop of de-ionized water filling the gap, a $Pt/H_2O/Ag$ cell was formed. In this work, the voltage polarity is stated with respect to the Ag electrode as the reference.

The electrical tests of $Pt/H_2O/Ag$ cells were carried out by an Agilent B1500A semiconductor device analyzer (Agilent Technologies, CA). Resistive switching was achieved for $Pt/H_2O/Ag$ cells. Figure 1 shows the bipolar hysteretic *I-V* characteristics of a cell with a Pt/Ag gap of 0.65 μm. The cell was switched on at ~−0.28 V with a cur-

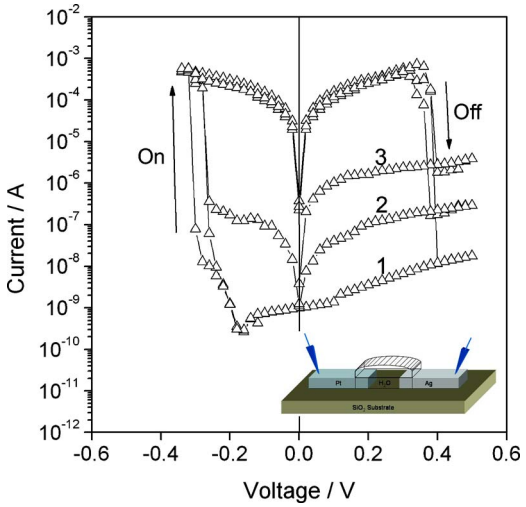

FIG. 1. Hysteretic *I-V* curves of a $Pt/H_2O/Ag$ cell with a Pt/Ag gap of 0.65 μm. A full voltage sweeping cycle follows this sequence: 0 V→−0.5 V→0 V→+0.5 V→0 V, and the cycle numbers are given in the figure. The voltage sweeping step was set to be 0.02 V/ 0.5 s. The inset is the sketch of a coplanar $Pt/H_2O/Ag$ cell.

[a]Author to whom correspondence should be addressed. Tel.:+49-2461-616074. FAX:+49-2461-612550. Electronic mail: x.guo@fz-juelich.de and guo@iwe.rwth-aachen.de

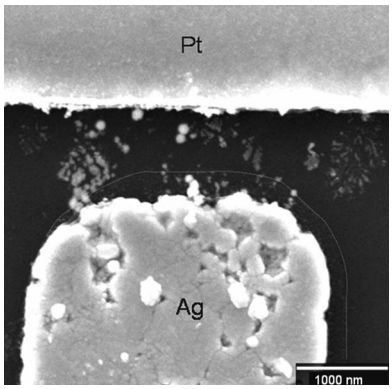

FIG. 2. SEM image of a $Pt/H_2O/Ag$ cell after resistive switching (on state). The dotted line indicates the original size of the Ag electrode.

rent jump of approximately five orders of magnitude, and switched off at ~0.37 V. Owing to the 1 mA current compliance, the relatively large heat capacity and the convection and evaporation of water, the effect of Joule heating is minimized. Similar resistive switching was achieved for $Pt/H_2O/Ag$ cells with Pt/Ag gaps up to 100 μm. Metallic Ag dendrites were formed between the Pt and the Ag electrodes, as demonstrated by scanning electron microscope (SEM) (type: Hitachi S-4100) image given in Fig. 2. Originally, the Pt/Ag gap was ~0.65 μm; however, a portion of the Ag electrode was dissolved during switching, then the gap increased to ~0.93 μm.

The switching-on process is illustrated in Fig. 3. After applying −1 V to a $Pt/H_2O/Ag$ cell with a Pt/Ag gap of 3 μm for about 4 s, the cell was switched on [Fig. 3(a)]. Therefore, −1 V was applied to cells of the same structure for 1, 2, and 4 s, respectively, and the cells were investigated by SEM afterwards. According to Figs. 3(b)–3(d), metallic dendrites grew from the Pt electrode toward the Ag electrode. *In situ* observations of the dendrite growth in a $Pt/H_2O/Ag$ cell with a Pt/Ag gap of 100 μm by an optical microscope disclosed a very similar situation. The dendrite growth rate was estimated to be ~1 μm/s.

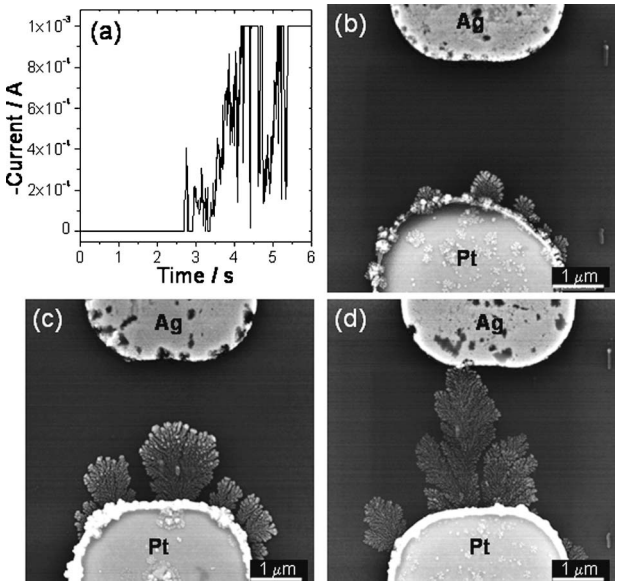

FIG. 3. The switching-on process while applying −1 V to a $Pt/H_2O/Ag$ cell with a Pt/Ag gap of 3 μm: (a) *I-t* curve, [(b), (c), and (d)] SEM images showing the Ag dendrite growth after applying −1 V for about 1, 2, and 4 s, respectively.

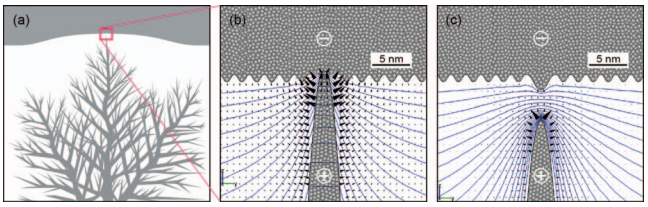

FIG. 4. (Color) Field simulation results of the front-most Ag dendrite and the Ag electrode during switching-off: (a) Sketch of the Ag dendrite and the solid Ag electrode. (b) Tip of the Ag dendrite in higher magnification, representing the situation in the late on state. The blue lines represent equal potential lines after applying a switching-off voltage of 200 mV. The voltage difference between two adjacent lines is 10 mV. The black cones represent the electrical field and point to the direction of the Ag^+ ion migration. (c) The situation slightly later, representing the early off-state. The Ag dendrite retreats due to the dissolution of Ag. As soon as the electrical contact is disconnected, the field distribution changes, which accelerates the further dissolution of the dendrite tip.

Upon applying a negative voltage, the switching-on process consists of the following steps: (1) metallic Ag is oxidized to Ag^+ ions at the Ag electrode/H_2O interface according to the reaction $Ag \rightarrow Ag^+ + e'$, (2) Ag^+ ions migrate through H_2O to the Pt electrode due to the potential difference between the Ag and the Pt electrodes, and (3) at the Pt electrode/H_2O interface, Ag^+ ions are reduced back to metallic Ag according to the reaction $Ag^+ + e' \rightarrow Ag$. As a consequence, metallic Ag dendrites grow from the Pt electrode toward the Ag electrode. During the switching-on process, the Ag electrode retreats as well, as a result of its dissolution. However, this process is minor because of the solid nature of the Ag electrode, in contrast with the dendrite twigs. In the moment when the front-most Ag dendrite tends to make the metallic contact to the solid Ag electrode, there are considerable fluctuations; therefore, the electrical current flowing through the cell oscillates significantly, as indicated in Fig. 3(a).

The dendrite morphology is fractal. The front-most dendrite twigs will probably be a few nanometers in width. Unfortunately, atomic force microscopy and high-resolution SEM failed to disclose the very fine fractal structure of the dendrite front. Due to the continuous dendrite growth, the Ag^+ ions are depleted in the region immediately in front of the dendrite. Under the influence of the electrical field between the dendrite and the Ag electrode, the dendrite continues to grow. However, once the dendrite front comes into contact with the Ag electrode, the current compliance sets in; the electrical field between the dendrite and the solid counterelectrode immediately drops to a significantly lower level. Then the driving force for the growth of the other dendrites decreases, and they (almost) stop growing. For this reason, there will be most probably just one dendrite twig that establishes the contact. The twig in contact with the Ag electrode is the weakest part and has the largest electrical resistance in the dendrite. The fine fractal structure of the dendrite is sketched in Fig. 4(a).

After switching on, the cell now becomes Pt/Ag dendrite (H_2O)/Ag, with a metallic Ag bridge (i.e., contacting twig). We assume that the contact point is only a few nanometers wide because such a contact is sufficient to establish the low resistance state and to activate the current compliance. Obviously, an originally asymmetric $Pt/H_2O/Ag$ cell becomes chemically symmetric because two Ag electrodes are involved at the contact point. However, the cell actually remains highly asymmetric in a morphological sense. On the

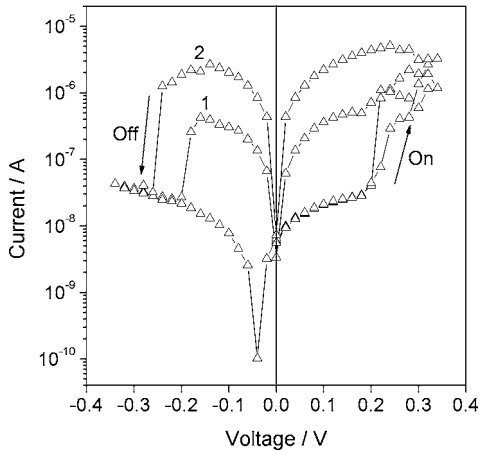

FIG. 5. Hysteretic *I-V* curves of an $Ag/H_2O/Ag$ cell with a Ag/Ag gap of 3 μm. The voltage sweeping step was set to be 0.02 V/1 s. The cycle numbers are given in the figure.

microscopic level, the contacting twig and the approximately planar Ag counterelectrode are extremely different in their curvatures. On a macroscopic level, this corresponds to a huge difference in volume density between the Ag dendrite and the Ag electrode.

Upon applying a reversed (i.e., positive) voltage to the Pt electrode, the switching-off process starts, which proceeds as follows: In parallel to the electronic current across the Ag twig, the positive voltage drop activates the oxidation reaction, $Ag \rightarrow Ag^+ + e'$, on all dendrite surfaces with a positive potential, while the electrochemical reduction and deposition takes place on the Ag electrode surface with a negative potential. A numerical field simulation using the software COMSOL™ was used to determine the equal potential lines and the field vectors in the vicinity of the twig. As shown in Fig. 4(b), the major voltage drop is located at the neck where the twig touches the planar Ag electrode. This leads to the dissolution of the bridge very near the neck position. Because of the tiny volume of the twig, a significant length of the dendrite is easily dissolved, while the redeposition takes place at the Ag electrode, so that the geometric front of the electrode only moves insignificantly toward the rapidly retreating dendrite front [Fig. 4(c)]. As a result, the gap between the Ag electrode and the Ag dendrite increases, and the cell is switched off. Before it is dissolved, the current density in the neck may reach very high values. Therefore, thermal effects and electromigration in the contacting neck, in principle, may occur. We have demonstrated that these effects do not play a dominant role in the switching-off process by varying the current compliance from a few 10 nA to 10 mA in comparable systems. Above 10 mA thermal effects are more likely to affect the process.

Obviously, the critical reason for the switching off lies in the fact that the curvature of the dendrite twig is much larger, and the cross-sectional area of the dendrite is orders of magnitude smaller than that of the Ag electrode. In order to test this idea, the *I-V* characteristics of symmetric $Ag/H_2O/Ag$ cells were measured. Typical results are given in Fig. 5. As shown in this figure, the cell was switched on and off in bipolar characteristics, despite its symmetric chemical nature. The geometric asymmetry of the cell was established in the first switching-on cycle, during which Ag dendrites evolved on the negative electrode. When the bias polarity was reversed, the $Ag/H_2O/Ag$ cell was switched off due to the curvature and dimension difference between the Ag dendrite and the Ag electrode.

In conclusion, bipolar resistive switching was reproduced for $Pt/H_2O/Ag$ cells. The switching-on process consists of the following steps: oxidation of metallic Ag, migration of Ag^+ ions to the Pt electrode, and reduction of Ag^+ ions on the Pt electrode. Ag dendrites grow from the Pt electrode toward the Ag electrode. Once the front-most dendrite contacts the Ag electrode, the cell is switched on. The switching-off process sets in when the voltage is reversed. It starts by the electrochemical dissolution of Ag atoms in the contacting dendrite. A numerical simulation shows that the dissolution starts at the neck where the dendrite contacts the solid surface, leading to a fast retreating of the dendrite. The tremendous curvature difference between the dendrite and the planar Ag bulk constitutes the reason for the bipolar switching of the cell. The switching on/off mechanism proposed in our model cells is especially meaningful for the bipolar resistive switching observed in ionic/mixed conductors.

When exposed to the ambient atmosphere, a water adsorption layer is almost always formed on the exposed objects. The adsorbed water layer may play an important role in the resistive switching observed in some cases reported in literatures.

Helpful discussions with Dr. G. Staikov and Professor W. Schmickler are appreciated.

[1] R. Dong, D. S. Lee, W. F. Xiang, S. J. Oh, D. J. Seong, S. H. Heo, H. J. Choi, M. J. Kwon, S. N. Seo, M. B. Pyun, M. Hasan, and H. Hwang, Appl. Phys. Lett. **90**, 042107 (2007).
[2] J.-W. Park, J.-W. Park, D.-Y. Kim, and J.-K. Lee, J. Vac. Sci. Technol. A **23**, 1309 (2005).
[3] Y.-H. You, B. S. So, J.-H. Hwang, W. Cho, S. S. Lee, T.-M. Chung, C. G. Kim, and K.-S. An, Appl. Phys. Lett. **89**, 222105 (2006).
[4] D. S. Jeong, H. Schroeder, and R. Waser, Appl. Phys. Lett. **89**, 082909 (2006).
[5] M. Fujimoto, H. Koyama, M. Konagai, Y. Hosoi, K. Ishihara, S. Ohnishi, and N. Awaya, Appl. Phys. Lett. **89**, 223509 (2006).
[6] B. J. Choi, S. Choi, K. M. Kim, Y. C. Shin, C. S. Hwang, S.-Y. Hwang, S.-S. Cho, S. Park, and S.-K. Hong, Appl. Phys. Lett. **89**, 012906 (2006).
[7] S. Karg, G. I. Meijer, D. Widmer, and J. G. Bednorz, Appl. Phys. Lett. **89**, 072106 (2006).
[8] Y. Watanabe, J. G. Bednorz, A. Bietsch, Ch. Gerber, D. Widmer, A. Beck, and S. J. Wind, Appl. Phys. Lett. **78**, 3738 (2001).
[9] K. Szot, W. Speier, G. Bihlmayer, and R. Waser, Nat. Mater. **5**, 312 (2006).
[10] M. P. Singh, L. Mechin, W. Prellier, and M. Maglione, Appl. Phys. Lett. **89**, 202906 (2006).
[11] R. Oligschlaeger, R. Waser, R. Meyer, S. Karthäuser, and R. Dittmann, Appl. Phys. Lett. **88**, 042901 (2006).
[12] A. Beck, J. G. Bednorz, Ch. Gerber, C. Rossel, and D. Widmer, Appl. Phys. Lett. **77**, 139 (2000).
[13] X. Chen, N. Wu, J. Strozier, and A. Ignatiev, Appl. Phys. Lett. **89**, 063507 (2006).
[14] A. Baikalov, Y. Q. Wang, B. Shen, B. Lorenz, S. Tsui, Y. Y. Sun, Y. Y. Xue, and C. W. Chu, Appl. Phys. Lett. **83**, 957 (2003).
[15] S. Tsui, A. Baikalov, J. Cmaidalka, Y. Y. Sun, Y. Q. Wang, Y. Y. Xue, C. W. Chu, L. Chen, and A. J. Jacobson, Appl. Phys. Lett. **85**, 317 (2004).
[16] M. Fujimoto, H. Koyama, S. Kobayashi, Y. Tamai, N. Awaya, Y. Nishi, and T. Suzuki, Appl. Phys. Lett. **89**, 243504 (2006).
[17] M. N. Kozicki, IEEE Trans. Nanotechnol. **4**, 331 (2005).
[18] M. Mitkova and M. N. Kozicki, J. Non-Cryst. Solids **299-302**, 1023 (2002).
[19] K. Terabe, T. Hasegawa, T. Nakayama, and M. Aono, Nature (London) **433**, 47 (2005).
[20] S. Kaeriyama, T. Sakamoto, H. Sunamura, M. Mizuno, H. Kawaura, T. Hasegawa, K. Terabe, T. Nakayama, and M. Aono, IEEE J. Solid-State Circuits **40**, 168 (2005).